

**Technical evaluation of Siemens  
Mammomat Inspiration digital breast  
tomosynthesis system**

**NHSBSP Equipment Report 1306  
version 2**

January 2015

Available from the National Co-ordinating Centre  
for the Physics of Mammography (NCCPM)

# About the NHS Cancer Screening Programmes

The national office of the NHS Cancer Screening Programmes is operated by Public Health England. Its role is to provide national management, coordination and quality assurance of the three cancer screening programmes for breast, cervical and bowel cancer.

The NHS Cancer Screening Programmes are part of Public Health England (PHE), an executive agency of the Department of Health.

[www.gov.uk/phe](http://www.gov.uk/phe)

## Lead authors:

CJ Strudley, LM Warren, KC Young

© Crown copyright 2015

You may re-use this information (excluding logos) free of charge in any format or medium, under the terms of the Open Government Licence v3.0. To view this licence, visit [OGL](http://www.ogil.gov.uk) or email [psi@nationalarchives.gsi.gov.uk](mailto:psi@nationalarchives.gsi.gov.uk). Where we have identified any third party copyright information you will need to obtain permission from the copyright holders concerned. Any enquiries regarding this publication should be sent to Mary Greatorex: [mary.greatorex@phe.gov.uk](mailto:mary.greatorex@phe.gov.uk)

Published: January 2015

PHE publications gateway number: 2014633



Document Information	
<b>Title</b>	Technical evaluation of Siemens Mammomat Inspiration digital breast tomosynthesis system
<b>Policy/document type</b>	Equipment Report 1306
<b>Electronic publication date</b>	January 2015
<b>Version</b>	2
<b>Superseded publications</b>	Version 1
<b>Review date</b>	None
<b>Author/s</b>	CJ Strudley LM Warren KC Young
<b>Owner</b>	NHSBSP
<b>Document objective (clinical/healthcare/social questions covered)</b>	To provide an evaluation of this equipment's suitability for use within the NHSBSP
<b>Population affected</b>	Women eligible for routine and higher-risk breast screening
<b>Target audience</b>	Physicists, radiographers, radiologists
<b>Date archived</b>	Current

# Contents

Contents	4
Acknowledgements	5
Executive summary	6
1. Introduction	7
1.1 Testing procedures and performance standards for digital mammography	7
1.2 Objectives	7
2. Methods	8
2.1 System tested	8
2.2 Dose and contrast to noise ratio under AEC	10
2.3 Image quality measurements	12
2.4 Geometric distortion and reconstruction artefacts	13
2.5 Alignment	15
3. Results	16
3.1 Output and HVL	16
3.2 Dose and CNR	16
3.3 Image quality measurements	21
3.4 Geometric distortion and resolution between focal planes	22
3.5 Alignment	26
4. Discussion	28
4.1 Dose and CNR	28
4.2 Image quality	28
4.3 Geometric distortion and reconstruction artefacts	29
4.4 Alignment	30
5. Conclusions	31
References	32

## Acknowledgements

The authors are grateful to the staff at Derriford Hospital, Plymouth, for their assistance during the evaluation of the unit at their site.

The contribution made by P Looney of the National Coordinating Centre for the Physics of Mammography (NCCPM), who wrote software for the data analysis, is also acknowledged.

Available from the National Co-ordinating Centre  
for the Physics of Mammography (NCCPM)

## Executive summary

The technical performance of the Siemens Mammomat Inspiration digital breast tomosynthesis system was tested in both 2D and tomosynthesis modes. 2D performance met current NHSBSP standards for digital mammography. No performance standards have yet been set for digital breast tomosynthesis systems.

The mean glandular dose to the standard breast was measured in tomosynthesis mode and found to be within the dose limits for 2D mammography. This report also provides baseline measurements on other aspects of the equipment performance, including image quality, noise, spatial distortion and alignment.

Available from the National Co-ordinating Centre  
for the Physics of Mammography (NCCPM)

# 1. Introduction

## 1.1 Testing procedures and performance standards for digital mammography

Testing procedures and performance standards for conventional 2D mammography are well established and documented<sup>1,2</sup> but there were not at the time of testing any nationally agreed procedures and standards for digital breast tomosynthesis (DBT) systems. The tests of tomosynthesis performance employed for this evaluation were based on those used for the TOMMY trial.<sup>3</sup> A national QC testing protocol has since been published.<sup>4</sup>

The technical performance of a 2D Siemens Mammomat Inspiration system has previously been assessed and reported.<sup>5</sup> For this evaluation, some of the tests in 2D mode were repeated.

Research to assess the clinical effectiveness of tomosynthesis is ongoing and further work will be required to establish measures of technical performance which indicate acceptable clinical performance. The results of these tomosynthesis performance tests may allow comparisons between different systems to be made, but should be interpreted with caution until further experience in the evaluation of tomosynthesis performance has been gained.

## 1.2 Objectives

This evaluation of the Siemens Mammomat Inspiration tomosynthesis system had two objectives. The first was to establish whether its 2D performance met the main standards in the NHSBSP and European protocols. The second was to provide baseline measurements on the performance of the system in tomosynthesis mode.

## 2. Methods

### 2.1 System tested

The Inspiration tested was an existing 2D system that had been upgraded to perform digital breast tomosynthesis (DBT). It employs a tungsten target with a rhodium filter for both conventional 2D and tomosynthesis imaging. (A molybdenum target and molybdenum filter are also available for 2D exposures). Tomosynthesis exposures are performed using a large format paddle which is exclusively for use in tomosynthesis. The breast support table is not flat and horizontal but slopes very slightly down towards the chest wall edge and towards the left and right sides.

Two automatic exposure control (AEC) modes are available for both 2D and tomosynthesis:

- *OpDose*, which selects beam quality, based on the compressed breast thickness (CBT), with automatic selection of the tube load. This mode can be used with *Segmentation* either on or off. *Segmentation* is a facility which adjusts exposures to optimise the imaging of denser areas
- *AEC*, in which the user selects the beam quality, with automatic selection of the tube load

In tomosynthesis, for both automatic modes, a preliminary stationary 2D exposure is always acquired, at a tube angle of zero degrees. This pre-pulse, with a tube load of 5mAs, is used to calculate the tube load for the tomosynthesis exposure.

There is also a manual mode in which the operator can manually select the tube load for a tomosynthesis exposure.

During a tomosynthesis acquisition the X-ray tube rotates about a centre of rotation which is 30mm above centre of the breast support table. The tube moves to a starting position at a tube angle of zero degrees, and the pre-pulse is performed with the tube stationary. The tube then moves into position, starting at an angle of approximately  $-25^{\circ}$  for the first projection. 25 projections are acquired, at intervals of approximately two degrees, with the tube in motion. The calculated tube load is divided equally between the projections. Collimation is dynamic and adjusts during the tomosynthesis acquisition to restrict the radiation field to the detector, which remains stationary. The grid is not used during tomosynthesis.

As well as acquiring 2D images or tomosynthesis images separately, the system can perform a '2D / 3D' exposure, in which a 2D view is followed by a tomosynthesis exposure, during the same compression.



*OpDose* mode was used to select the beam quality for all the tests which involved automatic selection of exposure factors. *Segmentation* was then turned off, which allowed the system to switch into *AEC* mode, while retaining the selected beam quality settings. (*Segmentation* is not appropriate for use when imaging QC phantoms.) The system tested had the standard *AEC* dose setting for 2D, with the dose for tomosynthesis set at approximately double the 2D dose.

For this evaluation, images were acquired using the *Physics QC Raw* format. This produces three types of image for each tomosynthesis exposure: raw projections, processed projections and reconstructed planes.

Reconstructed planes are 1mm apart, and the number reconstructed is the CBT in mm +1. A maximum of 100 planes can be reconstructed. If a tomosynthesis scan is performed on a greater thickness, a warning is given that only the bottom 100mm will be reconstructed.

Details of the system tested are given in Table 1.

**Table 1. System description**

Manufacturer	Siemens
Model	Mammomat Inspiration
System serial number	006-SPH0029230
Target material	Tungsten
Added filtration	50µm rhodium
Detector type	Amorphous selenium
Pixel size	85µm
Detector area	240mm x 300mm
Pixel array	2816 x 3584
Pixel value offset	50
AEC Modes	OpDose, AEC
AEC pre-exposure pulse	5mAs
Tomosynthesis projections	25 equal dose projections at approximately 2° intervals from -25 to +25°
Reconstructed focal planes	Vertical intervals: 1mm Number of planes : CBT in mm +1 (maximum 100)
Software version	VB30B(VX14F) (SL103P104)V syngo VE32C SL34P39 VB30B(VX14F) SL103 PACK P104\Aws SW versions\Aws\device\ versions

QC images were downloaded from the acquisition workstation via a USB port. The tomosynthesis images were in the DICOM<sup>6</sup> CT format. Individual reconstructed focal planes or projections, as well as the complete set of images from the tomosynthesis exposure, could be selected for export. Typical image file sizes are shown in Table 2.

**Table 2. 2D and tomosynthesis image file sizes**

	Pixels per frame	Frame size (mm)	File size per frame (MB)	Frames per image	Total image file size (MB)
2D small format	2082 x 2800	177 x 238	11.4	1	11.4
2D large format	2800 x 3518	238 x 299	19.2	1	19.2
Tomosynthesis projections	2816 x 3584	239 x 305	19.7	26 for processing +26 for presentation (incl. pre-pulse)	1024
Tomosynthesis reconstructed focal planes	2728 x 3480*	232 x 296	18.5*	61 for 60 mm thickness	1129* for 60 mm thickness

\*The number of pixels and file size for focal planes is variable. The upper end of the range found during testing is given here.

## 2.2 Dose and contrast to noise ratio under AEC

Dose and contrast to noise ratio (CNR) were measured using the AEC to expose different thicknesses of Perspex (polymethylmethacrylate or PMMA). The mean glandular dose (MGD) was calculated for the equivalent breast thicknesses. For CNR measurements, a square of aluminium 0.2mm thick was included in the phantom.

### 2.2.1 Dose measurement

To calculate MGDs, measurements were made of half value layer (HVL) and tube output, over the clinically relevant range of kV and filter combinations. They were made with the paddle raised well above the ion chamber. Measurements have been made on another Siemens Mammomat Inspiration system, both with the compression paddle in contact with the ion chamber and with the paddle raised well above the ion chamber.

In both 2D and tomosynthesis modes, exposures of a range of thicknesses of PMMA were made under AEC (after using *OpDose* mode to select beam quality, with *Segmentation* off). Spacers were used to create an air gap between the top of the PMMA and the paddle to give the correct equivalent breast thickness corresponding to each thickness of PMMA. The spacers were positioned across the back edge of the phantom to avoid interference with the rest of the tomosynthesis image.

Doses in 2D mode were calculated as described in the UK protocol. Doses in tomosynthesis mode were calculated using the method described by Dance et al.<sup>7</sup> This is an extension of the established 2D method, using the equation:

$$D = K g c s T \quad (1)$$

Where  $K$  is the incident air kerma at the top surface of the breast, and  $g$ ,  $c$  and  $s$  are conversion factors. The additional factor,  $T$ , is derived by summing weighted correction factors for each of the tomosynthesis projections. Values of  $T$  are tabulated for the Siemens Mammomat Inspiration system for different compressed breast thickness.

The Dance method of calculating MGD uses a measured dose at the surface of the breast with the paddle in place, but the method described in the UK protocol differs in that dose is measured with the paddle raised well above the ion chamber. To allow comparisons to be made between systems, MGD results in this report are calculated with the paddle raised. A correction factor is provided, which may be used to obtain a more accurate calculation of MGD.

### 2.2.2 Contrast to noise ratio

For CNR measurements a 10mm x 10mm square of 0.2mm thick aluminium foil was included in the phantom described above, positioned 10mm above the table on the midline, 60mm from the chest wall edge.

CNR in the 2D images was assessed using 5mm x 5mm regions of interest (ROIs) positioned in the centre of the aluminium square and at two background positions at the chest wall and nipple sides of the square.

CNR in the tomosynthesis focal plane was measured using 5mm x 5mm ROIs placed at the same positions as for the 2D image, as shown in Figure 1. The CNR was measured in the focal plane containing the aluminium square and in two planes above and two further planes below. The result quoted is the average of the measurements from all five planes.

CNR was also assessed in the unprocessed tomosynthesis projections acquired for the above images, using a 5mm x 5mm ROI.

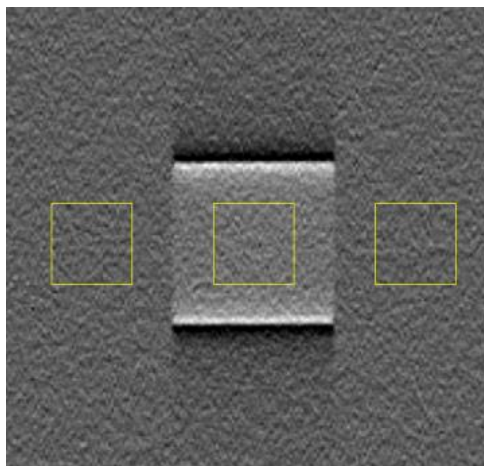


**Figure 1. The positioning of 5mm x 5mm ROIs for measurement of CNR in tomosynthesis**

Variation of tomosynthesis CNR with dose was assessed both in the projections and in the reconstructed image for an equivalent breast thickness of 53mm (that is, using a 45mm thickness of PMMA).

### 2.3 Image quality measurements

Image quality was assessed in 2D mode using a CDMAM phantom. In the absence of a more suitable test object for assessing tomosynthesis imaging performance, images of the CDMAM were also acquired in tomosynthesis mode. The CDMAM phantom (Version 3.4, serial number 1022) was sandwiched between two blocks of PMMA, each 20mm thick. The exposure factors used were the same as those selected by the AEC for an equivalent breast thickness of 60mm. One set of sixteen images was acquired in 2D mode at the AEC selected dose. In tomosynthesis mode, one set of sixteen images was acquired at the AEC selected dose and a further set at double this dose.

For the tomosynthesis exposures, the chest wall edge of the phantom was raised by 3mm so that the plane of the CDMAM would be parallel to the reconstructed focal planes in the reconstructed image (see geometric distortion results in section 3.4.1).

From the tomosynthesis images, the focal plane in best focus was selected. This was at the height of the CDMAM above the breast support table. The set of 2D images and the two sets of tomosynthesis images were read and analysed using two software tools, CDCOM version 1.6\* and CDMAM Analysis version 1.4.† This was repeated using the planes immediately above and

\*CDCOM version 1.6. Available from EUREF website: [www.euref.org](http://www.euref.org). Accessed 4 July 2013.

†CDMAM analysis UK v1.4, NCCPM, Guildford, UK

below the expected plane of best focus to ensure that the CDMAM result quoted corresponded to the best image quality obtained.

2D image quality assessed using the CDMAM is for an equivalent breast thickness of 60 mm. This can be related to the image quality at other thicknesses by using the CNRs measured for a range of thicknesses. The European protocol<sup>2</sup> gives the relationship between threshold contrast and CNR measurements, enabling calculation of a target CNR value for a particular level of image quality. This can be compared to CNR measurements for other breast thicknesses. Contrast for a particular gold thickness is calculated using Equation 2, and target CNR is calculated using Equation 3.

$$\text{Contrast} = 1 - e^{-\mu t} \quad (2)$$

where  $\mu$  is the effective attenuation coefficient for gold, and  $t$  is the gold thickness.

$$\text{CNR}_{\text{target}} = \frac{\text{CNR}_{\text{measured}} \times \text{TC}_{\text{measured}}}{\text{TC}_{\text{target}}} \quad (3)$$

where  $\text{CNR}_{\text{measured}}$  is the CNR for a 60mm equivalent breast,  $\text{TC}_{\text{measured}}$  is the threshold contrast calculated using the threshold gold thickness for a 0.1mm diameter detail (measured using the CDMAM at the same dose as used for  $\text{CNR}_{\text{measured}}$ ), and  $\text{TC}_{\text{target}}$  is the calculated threshold contrast corresponding to the threshold gold thickness required to meet either the minimum acceptable or achievable level of image quality.

The European protocol<sup>2</sup> also defines a limiting value for CNR, which is a percentage of the threshold contrast for minimum acceptable image quality for each thickness. The target CNR values for minimum acceptable and achievable levels of image quality and European limiting values for CNR were calculated.

## 2.4 Geometric distortion and reconstruction artefacts

The relationship between reconstructed tomosynthesis focal planes and the geometry of the volume that they represent was assessed. This was done by imaging a geometric test phantom consisting of a rectangular array of 1mm diameter aluminium balls, 50mm apart, in the middle of a 5mm thick sheet of PMMA. The phantom was placed at various heights (7.5, 32.5 and 57.5mm) within a 60mm stack of plain sheets of PMMA on the breast support table.

Reconstructed tomosynthesis planes were analysed to find the height of the focal plane in which each ball was best in focus, the position of the centre of the ball within that plane, the number of adjacent planes in which the ball was also seen, and to quantify the variation in appearance of the ball between focal planes.

This analysis was automated through the use of an ImageJ<sup>‡</sup> plug-in, developed by NCCPM for this purpose.

#### 2.4.1 Height of best focus

For each ball, the height of the focal plane in which it was best in focus was identified. Results were compared for all balls in each image, to determine whether there was any tilt of the test phantom relative to the reconstructed planes, or any vertical distortion of the focal planes within the image.

#### 2.4.2 Positional accuracy within focal plane

The x and y co-ordinates within the image were found for each ball. (The x and y directions are perpendicular and parallel to the chest wall edge, respectively). The mean distances between adjacent balls were calculated, using the pixel spacing quoted in the DICOM header. This was compared to the physical separation of balls within the phantom, to assess the scaling accuracy in the x and y directions. The maximum deviations from the mean x and y separations were calculated, to indicate whether there was any discernible distortion of the image within the focal plane.

#### 2.4.3 Appearance of the ball in adjacent focal planes

Changes to the appearance of a ball in different focal planes were assessed visually.

To quantify the extent of reconstruction artefacts in adjacent focal planes, the reconstructed image was treated as though it were a true three dimensional volume. The ImageJ plug-in was used to find the x, y, and z dimensions of a rectangular volume around each ball which enclosed all pixels with values exceeding 50% of the maximum pixel value. The method used was to create a composite x-y image using the maximum pixel values from all focal planes. A composite x line was then created using the maximum pixel from each column of the x-y composite plane. The full width at half maximum (FWHM) measurement in the x direction was made by fitting a polynomial spline. This was repeated in the orthogonal direction to produce the y-FWHM, and again using vertical re-sliced planes to find the z-FWHM. All pixel values were background subtracted, using the mean pixel value from around the ball in the plane of best focus. The composite z-FWHM thus calculated was used as a measure of the inter-plane resolution, or z-resolution. Its value would be different if a ball of different size were used.

The FWHM in the x and y directions of the image of the ball were also measured in the plane of best focus, in order to compare with the composite x- and y-FWHM measurements. This allowed quantification of any apparent shift or spread in the appearance of the ball through a series of adjacent focal planes.

---

<sup>‡</sup> <http://rsb.info.nih.gov/ij/>

## 2.5 Alignment

Alignment measurements were carried out for reconstructed tomosynthesis images.

The alignment of the X-ray beam to one focal plane of the reconstructed tomosynthesis volume was assessed at the height of the centre of rotation of the X-ray beam, 30mm above the surface of the breast support table. Self-developing film and graduated markers were supported at the required height and positioned on each edge of the X-ray beam. The alignment at the lateral edges could only be measured at this height because at other heights the movement of the tube during the scan would cause the lateral edges of the X-ray beam to move between projections.

The alignment of the imaged volume to the compressed volume was also assessed. Missed tissue at the chest wall edge was assessed at the height of the surface of the breast support table using a graduated marker. Small high contrast markers were placed on the breast support table and on the underside of the compression paddle to assess vertical alignment. The image planes were then inspected to determine whether all markers were brought into focus within the reconstructed volume.

Available from the National Co-ordinating Centre  
for the Physics of Mammography (NCCPM)

## 3. Results

### 3.1 Output and HVL

The tube output and HVL results are shown in Table 3. The paddle was in the beam and was raised well above the ion chamber. Measurements that had been made on another Siemens Mammomat Inspiration system, showed that the dose measured with the paddle in contact with the upper surface of the ion chamber was 4.5% higher than that measured with the paddle raised well above the ion chamber. A correction factor of 1.045 would therefore be applied to the output measurements in Table 3 and the MGDs in section 3.2, if scatter from the paddle were to be taken into account.

**Table 3. HVL and tube output measurement**

kV	Target	Filter	Tube output ( $\mu\text{Gy/mAs}$ at 1m)	HVL (mm)
25	W	Rh	8.93	0.52
28	W	Rh	12.5	0.55
31	W	Rh	15.9	0.58
34	W	Rh	19.3	0.61

### 3.2 Dose and CNR

The MGDs calculated for 2D and tomosynthesis modes are shown in Tables 4 and 5, and presented graphically in Figure 2. The correction factor of 1.045 has not been applied.

**Table 4. Dose and CNR for 2D images acquired under AEC**

PMMA (mm)	Equivalent breast thickness (mm)	kV	Target / filter	mAs	MGD* (mGy)	NHSBSP dose limit (mGy)	CNR
20	21	26	W / Rh	33	0.45	1.0	9.3
30	32	27	W / Rh	49	0.62	1.5	8.5
40	45	28	W / Rh	74	0.86	2.0	7.8
45	53	29	W / Rh	83	0.99	2.5	7.3
50	60	30	W / Rh	94	1.16	3.0	7.0
60	75	31	W / Rh	134	1.60	4.5	6.1
70	90	32	W / Rh	185	2.11	6.5	5.3

\*The mAs and MGD values quoted include the pre-exposure pulse (tube load 5mAs), which is not included in the image.



The CNR measurements for 2D images are shown in Table 4. Table 5 shows the measured CNRs for the reconstructed tomosynthesis images and for the central (zero degree) 2D projection images. The dose for an individual projection is 1/25 of the total dose from a tomosynthesis acquisition.

**Table 5. Dose and CNR for tomosynthesis images acquired under AEC**

PMMA (mm)	Equivalent breast thickness (mm)	kV	Target / filter	mAs*	MGD* (mGy)	CNR in reconstructed tomosynthesis image	CNR in central projection image
20	21	26	W / Rh	72	0.95	1.85	2.87
30	32	27	W / Rh	104	1.26	1.58	2.40
40	45	28	W / Rh	150	1.67	1.34	2.06
45	53	29	W / Rh	167	1.90	1.21	1.87
50	60	30	W / Rh	185	2.18	1.13	1.72
60	75	31	W / Rh	252	2.87	0.93	1.46
70	90	32	W / Rh	329	3.58	0.75	1.36

\*The mAs and MGD values quoted include the pre-exposure pulse (tube load 5mAs), which is not included in the reconstructed tomosynthesis image.

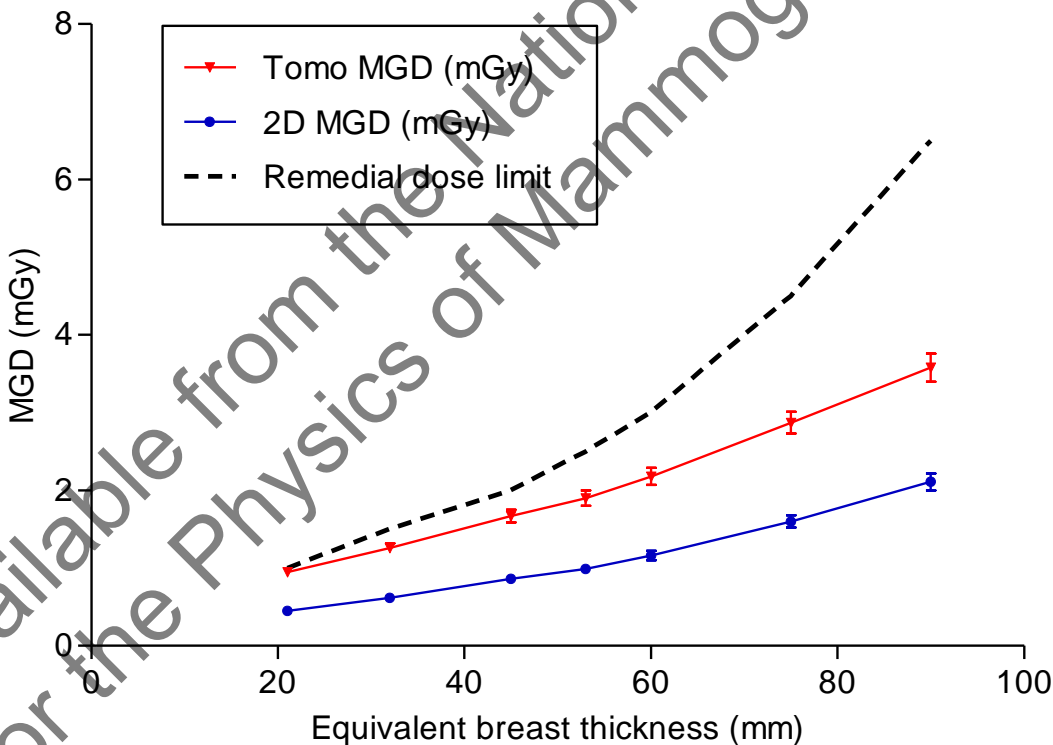


**Figure 2. MGD for 2D and tomosynthesis images under AEC. (Error bars indicate 95% confidence limits.)**

The CNR results for 2D and tomosynthesis are presented graphically in Figures 3 and 4. Figure 3 includes the target levels of CNR required to reach the minimum acceptable and achievable levels of 2D image quality (IQ), 5.0 and 7.3 respectively, for 0.1mm details. These were calculated using an equivalent attenuation coefficient of 0.125 for 30kV W/Rh. The European limiting values of CNR are also shown.

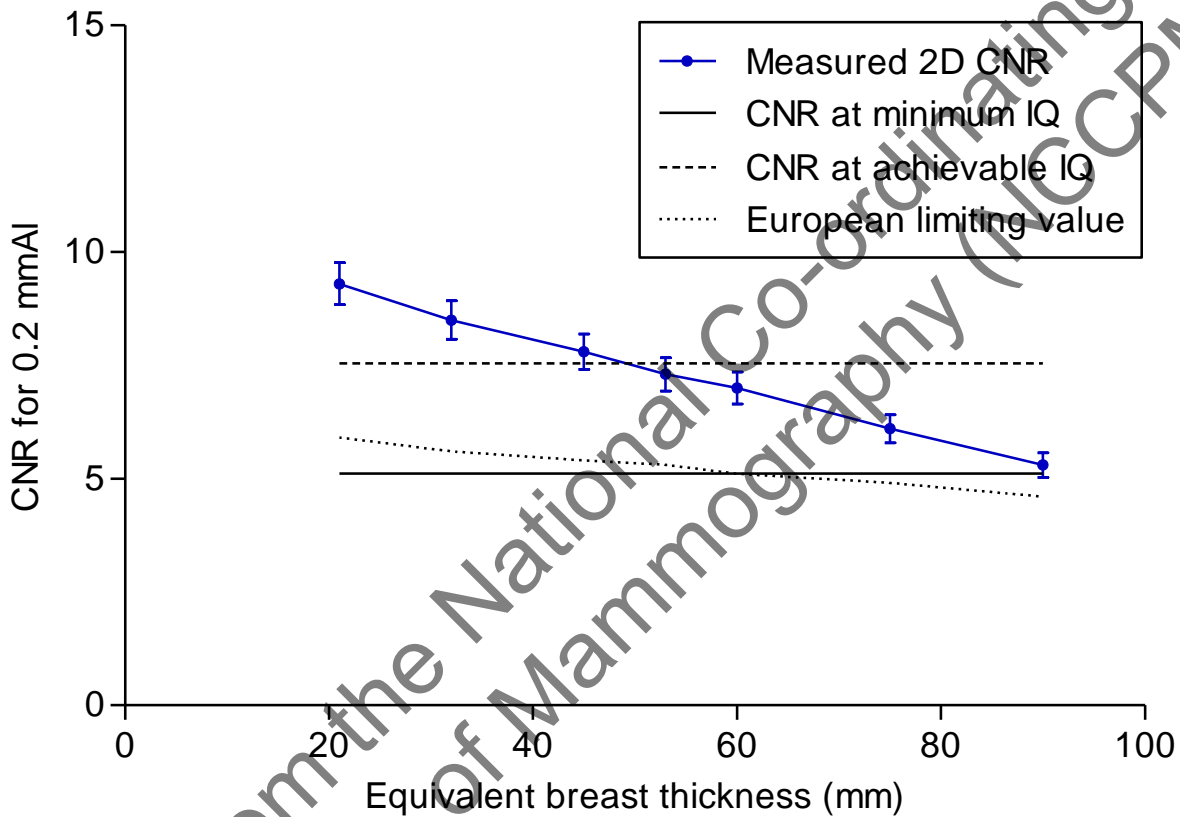
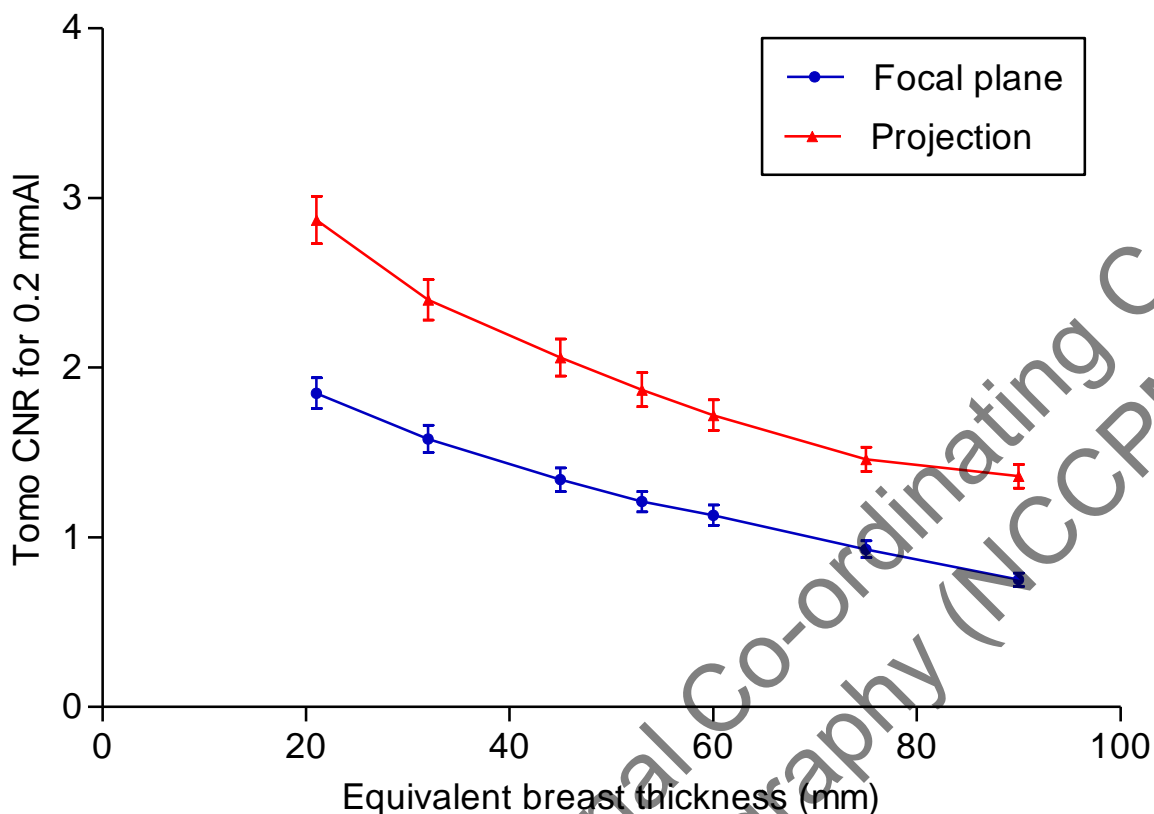


Figure 3. CNR for 2D images obtained under AEC compared with limiting values from the NHSBSP and European protocols. (Error bars indicate 95% confidence limits.)



**Figure 4. CNR for tomosynthesis images obtained under AEC. (Error bars indicate 95% confidence limits.)**

The variation of tomosynthesis CNR with dose is shown in Table 6 and Figure 5. A power fit was applied to the relationship between CNR and dose for reconstructed focal planes and projections.

Figure 6 shows the variation of projection CNR with tube angle for three thicknesses of PMMA.

**Table 6. Variation of tomosynthesis CNR with dose**

PMMA (mm)	Equivalent breast thickness (mm)	kV	Target / filter	mAs	MGD (mGy)	CNR in reconstructed DBT image	CNR in central projection
45	53	29	W / Rh	56	0.64	0.61	1.01
45	53	29	W / Rh	90	1.02	0.81	1.30
45	53	29	W / Rh	160	1.82	1.19	1.88
45	53	29	W / Rh	250	2085	1.49	2.37
45	53	29	W / Rh	560	6.38	2.31	3.59

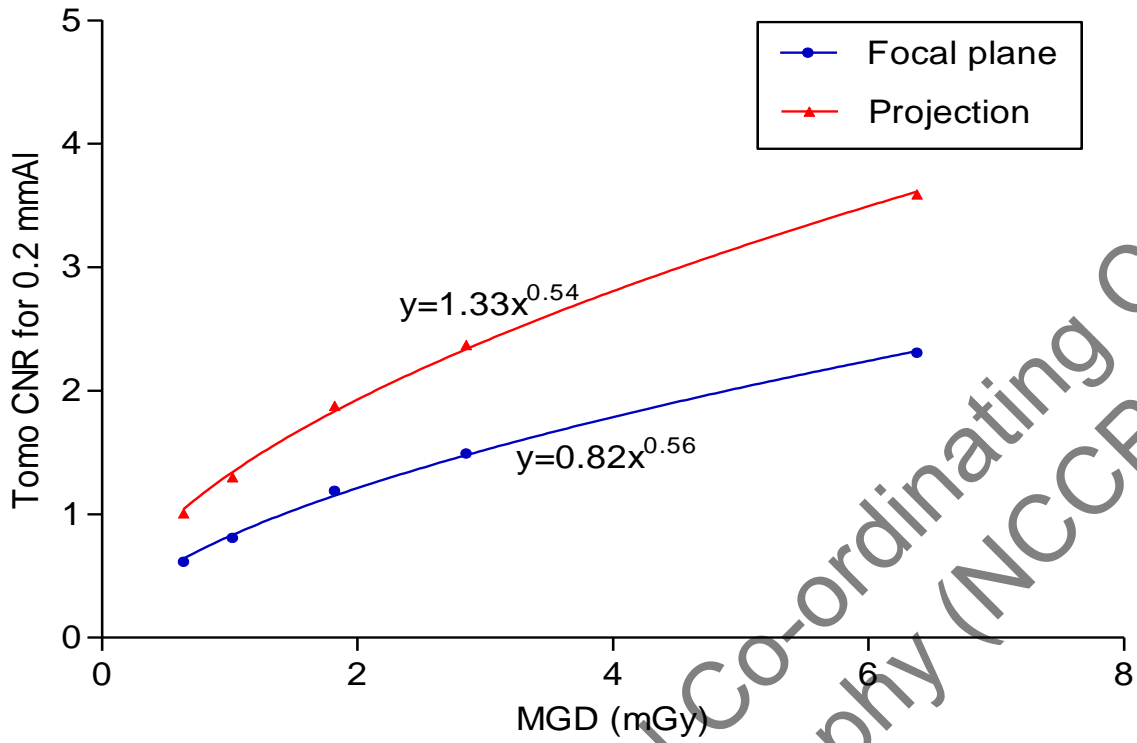


Figure 5. CNR measured in tomosynthesis mode, for a 53mm equivalent breast thickness at a range of doses. (Error bars indicate 95% confidence limits.)

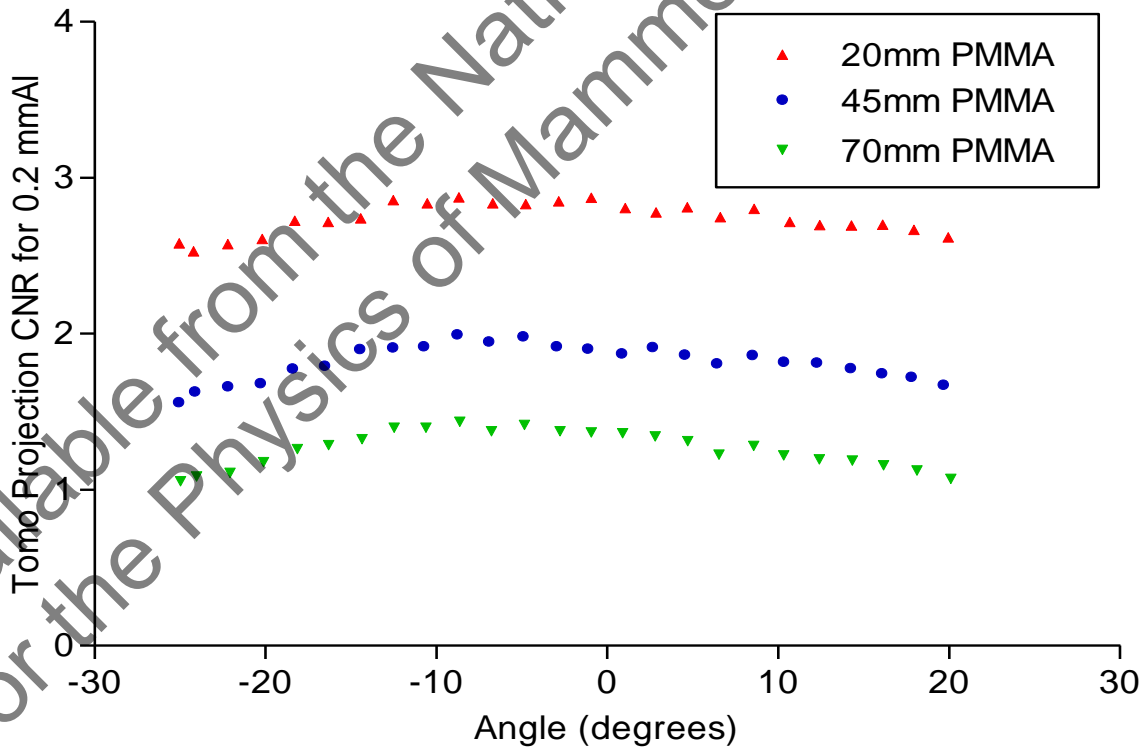


Figure 6. CNR measurements in tomosynthesis projections for three different PMMA thicknesses

### 3.3 Image quality measurements

The contrast detail curve for sixteen 2D images is shown in Figure 7.

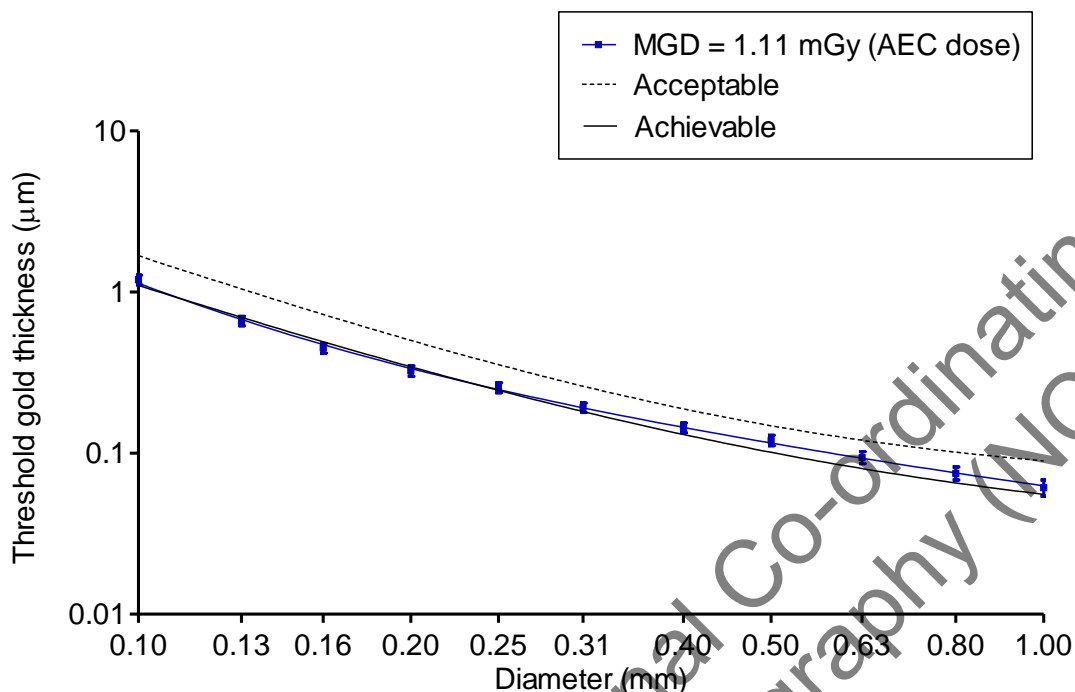


Figure 7. Threshold gold thicknesses for 2D images acquired at 30kV W/Rh. (Error bars indicate 95% confidence limits.)

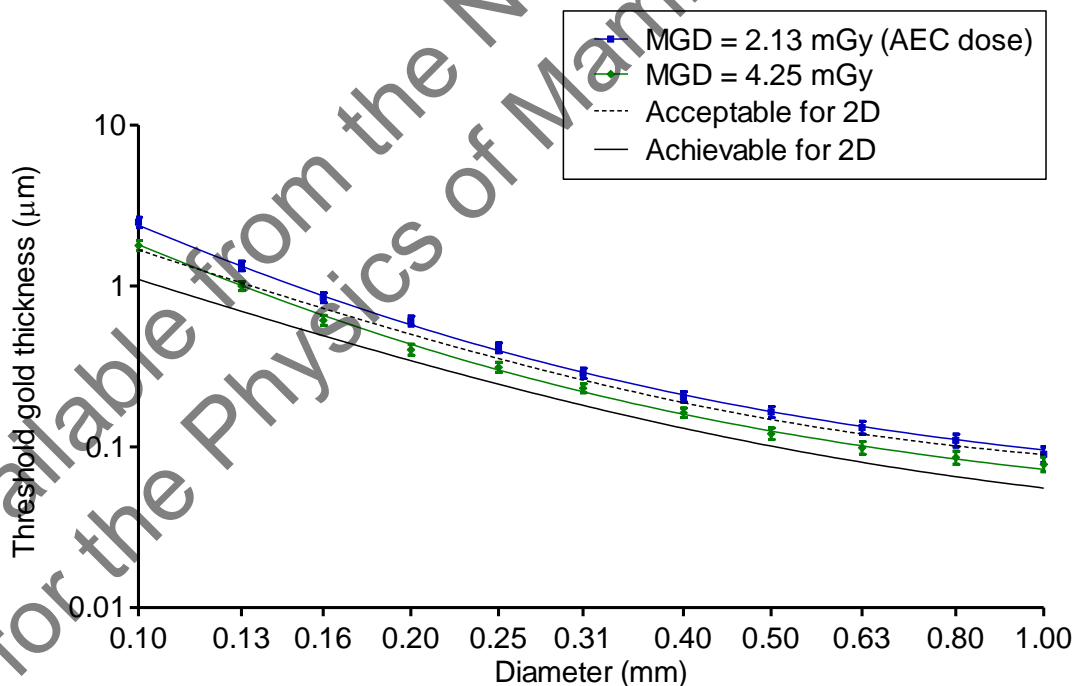


Figure 8. Threshold gold thicknesses for tomosynthesis images acquired at two doses, at 30kV W/Rh. (Error bars indicate 95% confidence limits.)

In Figure 8, CDMAM curves are shown for sets of 16 images, assessed using the plane in best focus from each set. Results are for the AEC selected dose and for twice this dose.

The image quality results shown in Figures 7 and 8 are summarised in Table 7.

**Table 7. Average threshold gold thicknesses for CDMAM images in 2D and tomosynthesis**

Detail diameter (mm)	Threshold gold thickness (µm)				
	2D AEC dose 1.11 mGy	DBT AEC dose 2.13mGy	DBT double AEC dose 4.25mGy	Minimum standard for 2D	Achievable standard for 2D
0.10	1.191	2.495	1.791	1.680	1.100
0.25	0.255	0.414	0.313	0.352	0.244
0.50	0.120	0.165	0.121	0.150	0.103
1.00	0.061	0.090	0.078	0.091	0.056

### 3.4 Geometric distortion and resolution between focal planes

#### 3.4.1 Height of best focus

For each of the three images, acquired at different heights, the height of best focus for each ball was found to increase with distance from the chest wall edge. The mean gradient was 0.018, corresponding to a height differential of 3mm over a distance of 170mm. This indicates that the reconstructed focal planes are aligned to the horizontal plane rather than to the slightly inclined surface of the breast support table.

At the chest wall edge of the image the height of best focus for each ball was found to be within 1mm of its height above the table. For each set of balls at the same distance from the chest wall edge the height variation was no greater than 1mm, indicating that the focal planes are flat and horizontal.

#### 3.4.2 Positional accuracy within focal plane

The mean distances between balls, calculated using the pixel spacings from the DICOM headers, were 50.0mm in both x and y directions. The true separation between balls was 50.0mm, indicating no scaling error in either direction. The maximum deviation from the mean separations was 0.1mm in both x and y directions, while the test object’s manufacturing specification was a non-cumulative positioning accuracy of ± 0.1mm. These results indicate that there is no discernible geometric distortion within the focal plane.

### 3.4.3 Appearance of the ball in adjacent focal planes

The image of a 1mm diameter aluminium ball is well defined in the plane of best focus, but appears flattened with a dark area (reduced pixel value) to either side in the y direction (parallel to the chest wall edge), as shown in the middle frame of the second row in Figure 9. In focal planes above and below, the image of the ball becomes longer and fainter, and stretches into a line, as shown in Figure 9. There is also a slight shift in the direction perpendicular to the chest wall edge. The views shown are taken at 1mm intervals, from 7mm below to 7mm above the plane at the same height as the ball.

Figure 10 shows the focal planes re-sliced into vertical planes in the x-z and y-z orientations.

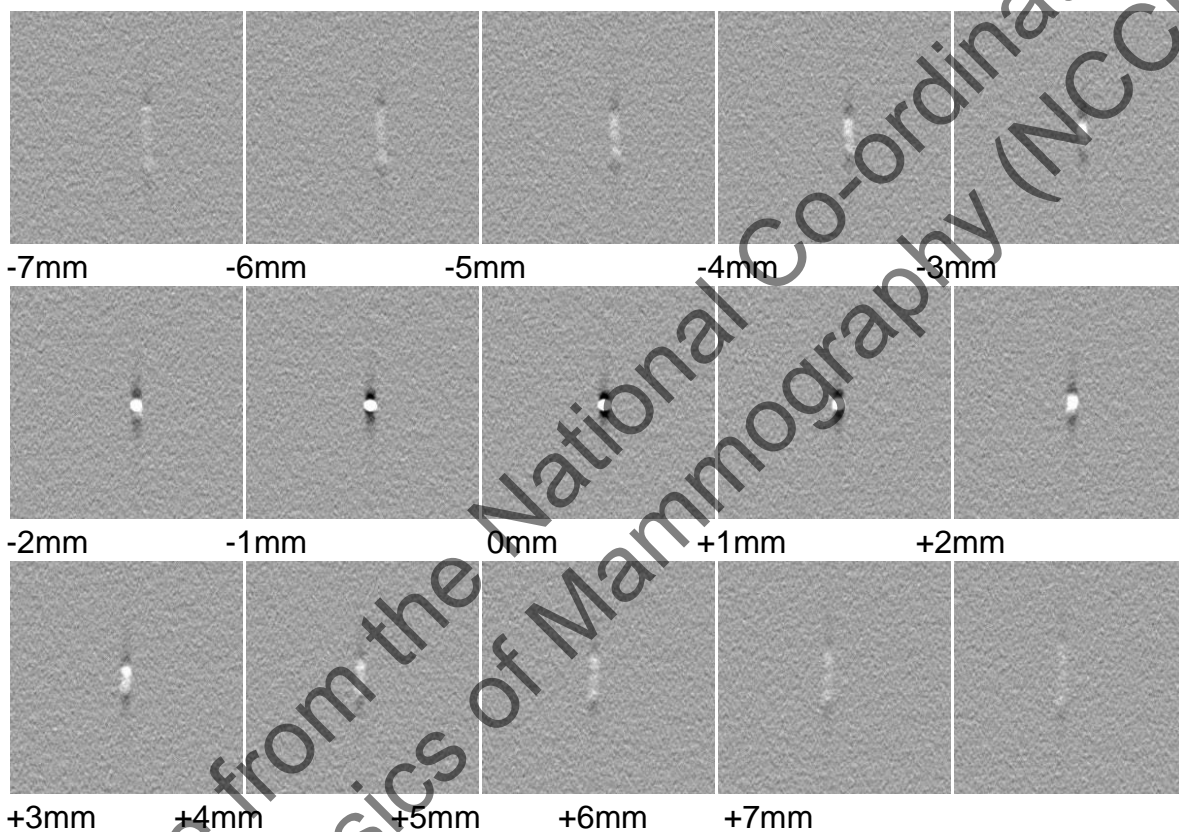


**Figure 9. Appearance in focal planes at different heights of a 1mm aluminium ball, 110mm from the chest wall edge, in the central area of a tomosynthesis image.**

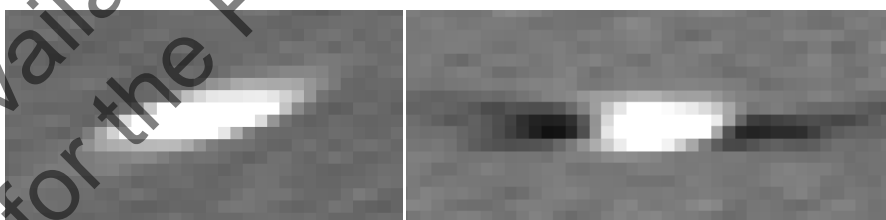


**Figure 10. Vertically resliced planes through the centre of a 1mm aluminium ball, 110mm from the chest wall edge, in the central area of a tomosynthesis image. The x-z plane is on the left and the y-z plane is on the right.**

Table 8 shows the results of the automated analysis of the images. The x- and y-FWHM from the plane of best focus, and the composite FWHM (from all planes) are shown. The difference between these quantities indicates the apparent shift or spread of the image between planes.

**Table 8. Mean dimensions and range (in brackets) of FWHM, for 1mm diameter aluminium balls and their associated reconstruction artefacts.**

	FWHM within plane of best focus (mm)	Composite FWHM using all planes (mm)	Apparent shift or spread between focal planes (mm)
x (perpendicular to chest wall edge)	0.89 (0.83 to 0.96)	1.14 (0.86 to 1.53)	0.26 (0.01 to 0.65)
y (parallel to chest wall edge)	0.71 (0.62 to 0.79)	0.85 (0.67 to 1.23)	0.14 (0.00 to 0.47)
z (vertical)		3.9 (3.6 to 4.3)	

The variations of the measurements for individual balls with position within the reconstructed image are presented graphically in Figures 11 to 13.

Figure 11 shows that the composite x-FWHM (in the direction perpendicular to the chest wall edge) increases with distance from the edge. Figure 12 shows that the composite y-FWHM increases with distance from the centre of the midline.

The composite z-FWHM measurements give a measure of the inter-plane or z-resolution for the tomosynthesis image. Figure 13 shows no significant dependence of z-FWHM on position within the image.



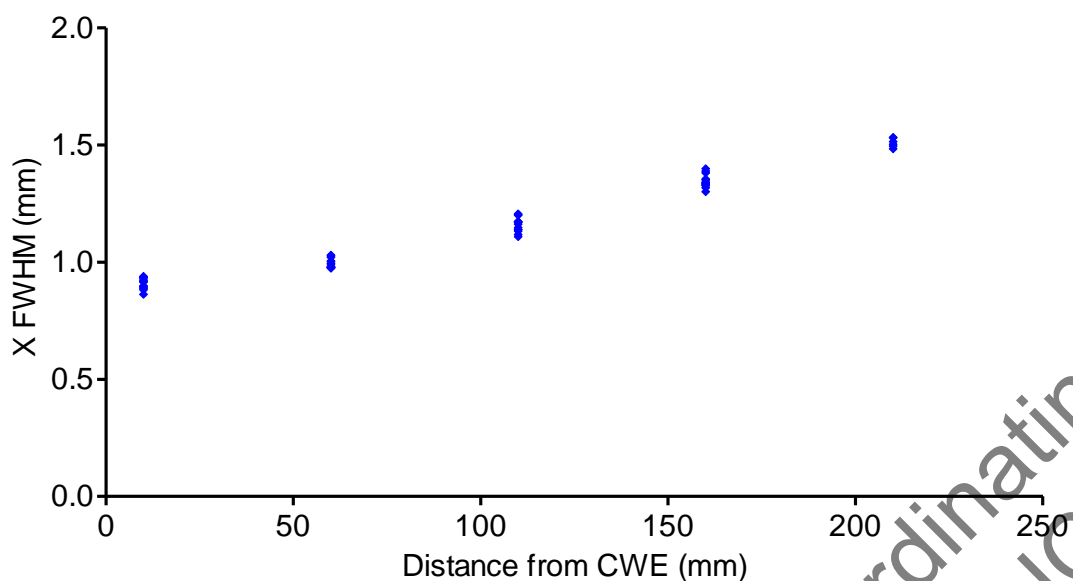


Figure 11. Composite FWHM in the x-direction (perpendicular to the chest wall edge) plotted against distance from the chest wall edge.

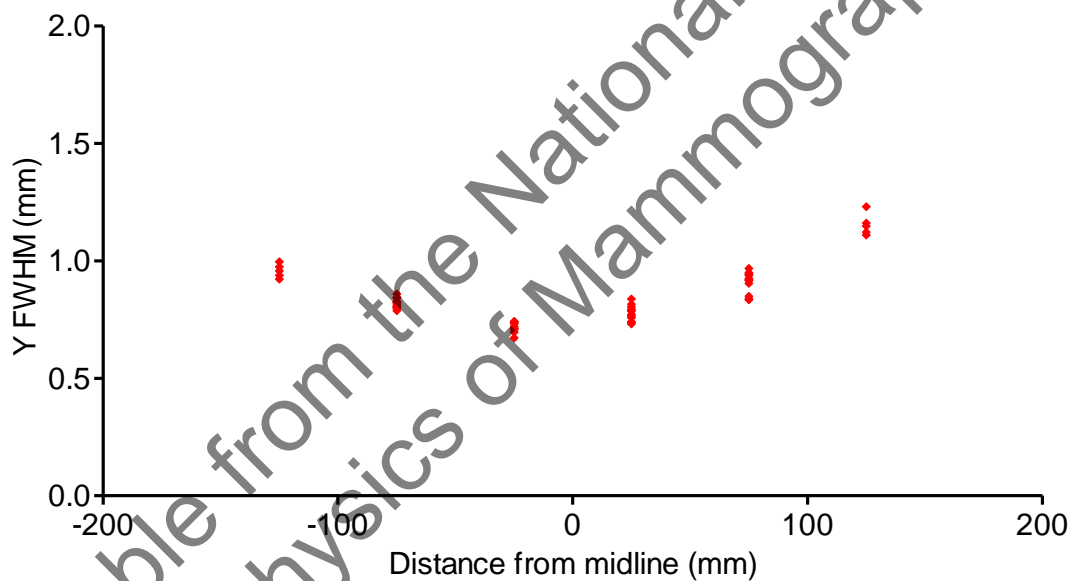
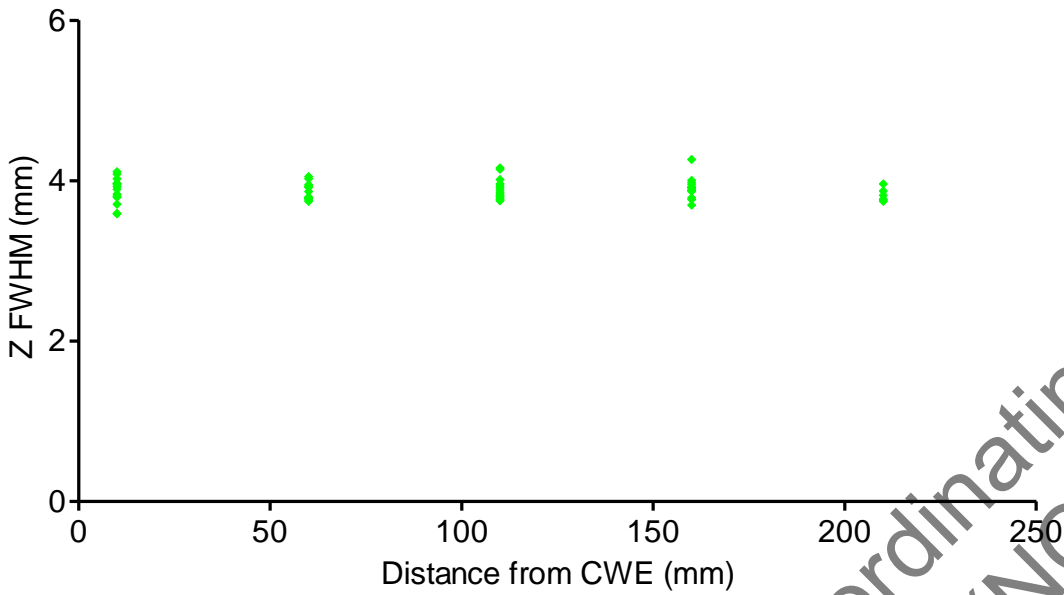


Figure 12. Composite FWHM in the y-direction (parallel to the chest wall edge) plotted against distance from the midline.



**Figure 13. Composite FWHM in the z- direction (vertical) plotted against distance from the chest wall edge.**

### 3.5 Alignment

Table 9 shows the alignment of the X-ray field to the reconstructed image at the height of the centre of rotation, 30mm above the surface of the breast support table. The X-ray field overlaps the edges of the reconstructed image by less than 5mm, which is the limit applied in 2D mammography.

**Table 9. Alignment of X-ray field to reconstructed tomosynthesis image**

Height above table (mm)	X-ray field to reconstructed tomosynthesis image* (mm)			
	Front	Back	Left	Right
0	1			
30	1.5	3	0	1
80	1			

\*A positive value indicates that the X-ray field overlaps the edge of the image

The alignment of the reconstructed volume to the compressed volume was assessed. The amount of missed tissue at the chest wall edge was 4mm at the surface of the breast support table. This is within the 5mm limit which is applied in 2D mammography.

All markers distributed in the central area of the surface of the breast support table and the underside of the compression paddle were brought into focus in planes near the bottom and top of the image. This showed that no details are missed at the base or top of the reconstructed volume in the central area. However, due to the slope of the breast support table (as noted in

section 3.4.1), it is anticipated that the lowest 2mm of tissue near the chest wall edge, will be left out of the reconstructed volume. The same may apply to a few mm of tissue at the top, as the compression paddle tends to tilt. Small details at the top and bottom of the chest wall edge will, therefore, not be brought into sharp focus in any focal plane.

Available from the National Co-ordinating Centre  
for the Physics of Mammography (NCCPM)

## 4. Discussion

### 4.1 Dose and CNR

The MGDs to the standard breast were calculated for a range of equivalent breast thicknesses from 20mm to 90mm. In both 2D and tomosynthesis modes the doses were well within the NHSBSP dose limits for 2D mammography (except for the smallest equivalent breast thickness, where the tomosynthesis dose is close to the limit). The MGD to a 53mm equivalent breast thickness was 0.99mGy and 1.90mGy for 2D and tomosynthesis respectively, while the NHSBSP dose limit for 2D mammography is 2.5mGy for this thickness.

In 2D mode under AEC, the CNR for all equivalent breast thicknesses exceeded the value required to meet the NHSBSP standard for minimum acceptable image quality. The CNR only exceeded the value required for the achievable level of image quality for equivalent breast thicknesses of less than 50 mm. This could be improved by increasing the dose under AEC. As usual in digital mammography, the CNR for 2D imaging decreased significantly as the breast thickness increased.

CNR values in reconstructed tomosynthesis focal planes are expected to be highly dependent on the degree of smoothing and scaling inherent within the reconstruction algorithm. Any interpretation of absolute CNR values in relation to image quality should therefore be treated with caution. The CNR measured in the focal plane is seen to decrease with breast thickness to a greater extent than the CNR measured in 2D. This may be largely due to the greater amount of scatter reaching the detector in the tomosynthesis projections in the absence of a grid.

CNR measurements were also made in the unprocessed tomosynthesis projections. The CNRs are lower because the dose per projection is a fraction (1/25) of the total dose in tomosynthesis. The CNR in projections decreased slightly with increasing projection angle. A variation would be expected due to the change in contrast and noise with increasing angle.

The variation of tomosynthesis CNR with dose was assessed. A power fit applied to the relationships between CNR and dose had an index close to 0.5 for both reconstructed focal planes and projections. This indicates that quantum noise is the dominant noise source in the tomosynthesis images.

### 4.2 Image quality

Image quality was assessed in 2D mode using the CDMAM test object under AEC. The 2D threshold gold thickness curve is close to (or a little less than) the achievable level of image quality for all detail sizes.

No suitable test object has yet been developed for assessing image quality in tomosynthesis. However, CDMAM images were acquired, under AEC, in tomosynthesis mode. The resulting

threshold gold thickness curve for tomosynthesis is poorer than the minimum acceptable level of image quality that is defined for 2D mammography. This result takes no account of the ability of tomosynthesis to remove the obscuring effects of overlying tissue in a clinical image. The degree of this effect in different tomosynthesis systems is expected to vary, depending on the angular range over which projections are acquired. The Inspiration, with a relatively wide angular range, may be very effective in removing the appearance of overlying tissues. This would compensate for the relatively poor CDMAM performance compared to 2D imaging. As expected, the threshold gold thickness decreased when the dose was doubled.

There is no standard test object available yet that would allow a realistic and quantitative comparison of image quality between tomosynthesis systems, or between 2D and tomosynthesis modes. A suitable test object would need to incorporate simulated breast tissue to show the benefit of removing overlying breast structure in tomosynthesis imaging, as compared to 2D imaging. In the absence of such a test object, an extensive clinical trial would be needed to determine whether the performance of a particular tomosynthesis system is likely to be clinically adequate.

### 4.3 Geometric distortion and reconstruction artefacts

Assessment of geometric distortion images demonstrated that reconstructed tomosynthesis focal planes are horizontal, rather than parallel to the slightly sloping surface of the breast support table. There was no vertical distortion. Within the focal plane, comparison of measured with nominal separations of imaged details demonstrated that there is no geometric distortion. There is no scaling error in using the pixel spacing quoted in the image DICOM headers.

In the *QC Raw* tomosynthesis images of 1mm aluminium balls within a PMMA block, the balls did not appear circular when viewed within the plane of best focus. Instead, they appeared flattened with a dark area (indicating reduced pixel value), to either side in the y-direction, that is, parallel to the chest wall edge. The excessive contrast produced by the aluminium ball is the cause of this artefact. However, it is not necessarily predictive of such artefacts in clinical images. These have less abrupt changes in contrast and additional image processing is applied. On viewing successive focal planes away from the plane of best focus, the image of a ball stretches into a line which fades and changes direction slightly. It also shifts position slightly in the direction perpendicular to the chest wall edge.

Within focal planes, the spread of reconstruction artefacts associated with balls increased with distance from the centre of the chest wall edge of the image. Due to the geometry of the diverging primary X-ray beam, the reconstruction artefacts might be expected to extend further away from the centre of the chest wall edge of the image with increasing distance from the X-ray tube focal spot. Measurement of the maximum extent of the 50% contour level in background corrected pixel values around each ball in all planes quantified the magnification effect between focal planes. This measurement exceeded that in the plane of best focus by up to 0.6mm.

A tomosynthesis system employing a wide range of projection angles, like the Inspiration, is expected to have good inter-plane resolution with little persistence between focal planes. The 50% contour extended vertically between focal planes, giving a mean inter-plane resolution of 4mm for the 1mm diameter balls. Balls of different diameter would result in more or less extensive reconstruction artefacts, so the inter-plane resolution would vary accordingly. Inter-plane resolution did not vary by any more than 10% with vertical or horizontal position of the balls.

#### 4.4 Alignment

It is not possible to assess the alignment of the irradiated volume to the imaged volume because the lateral parts of the volume are partially irradiated as the X-ray field moves during the tomosynthesis scan. At the height of the centre of rotation (30mm above the surface of the breast support table) the X-ray beam extended beyond the edges of the reconstructed focal plane by less than the 5mm limit which is applied to 2D mammography.

Assessment of the alignment of the tomosynthesis imaged volume to the compressed volume indicated that 4mm of tissue is missed at the chest wall edge at the height of the surface of the breast support table. This is within the 5mm limit for 2D mammography. There was no missed tissue in the central area at either the top or bottom of the reconstructed image. However, the table slopes down towards the chest wall edge, and the paddle may tilt slightly upwards during compression. It is therefore likely that a few mm of tissue at both top and bottom, near the chest wall edge, would not be brought into sharp focus.

## 5. Conclusions

The technical performance was tested in both 2D and tomosynthesis modes. 2D performance met current NHSBSP standards for digital mammography. No performance standards have yet been set for digital breast tomosynthesis systems and it is not yet possible to predict clinical tomosynthesis performance from these results.

The MGD to the standard breast was found to be almost twice as large in tomosynthesis mode as in 2D mode. Since doses on the Siemens Mammomat Inspiration are quite low in 2D, the doses in tomosynthesis are still well within the NHSBSP dose limits for 2D mammography. It would be desirable to increase the doses in 2D mode to improve image quality, especially for thicker breasts.

Available from the National Co-ordinating Centre  
for the Physics of Mammography (NCCPM)

## References

1. Kulama E , Burch A, Castellano I et al. *Commissioning and Routine Testing of Full Field Digital Mammography Systems* (NHSBSP Equipment Report 0604, Version 3). Sheffield: NHS Cancer Screening Programmes, 2009
2. Van Engen R, Young KC, Bosmans H et al. The European protocol for the quality control of the physical and technical aspects of mammography screening. In: *European Guidelines for Quality Assurance in Breast Cancer Screening and Diagnosis*, 4th Edition. Luxembourg: European Commission, 2006.
3. Strudley CJ, Young KC, Oduko JM et al. Development of a Quality Control Protocol for Digital Breast Tomosynthesis Systems in the TOMMY Trial. In: *International Workshop on Breast Imaging 2012*. Berlin: Springer-Verlag, 2012, 330–337.
4. Burch A, Loader R, Rowberry B et al. *Routine Quality Control Tests for Breast Tomosynthesis (Physicists)* (NHSBSP Equipment Report 1407). Sheffield: NHS Cancer Screening Programmes, 2014
5. Young KC, Oduko JM, Gundogdu O et al. *Technical Evaluation of Siemens Mammomat Inspiration Full Field Digital Mammography System* (NHSBSP Equipment Report 0909). Sheffield: NHS Cancer Screening Programmes, 2009
6. *Digital Imaging and Communications in Medicine (DICOM) Part 3: Information Object Definitions*. Virginia: National Electrical Manufacturers Association, 2011.
7. Dance DR, Young KC, van Engen RE. Estimation of mean glandular dose for breast tomosynthesis: factors for use with the UK, European and IAEA breast dosimetry protocols. *Physics in Medicine and Biology*, 2011, 56: 453-471.